Materials Letters 235 (2019) 184–188

Contents lists available at ScienceDirect

Materials Letters

journal homepage: www.elsevier.com/locate/mlblue

Enhanced sorption of Cu^{2+} from sulfate solutions onto modified electric arc furnace slag

Irena Nikolić [a,b,*], Smilja Marković [c], Ljiljana Veselinović [c], Vuk V. Radmilović [d], Ivona Janković-Častvan [e], Velimir R. Radmilović [e,f]

[a] University of Montenegro, Faculty of Metallurgy and Technology, Podgorica, Montenegro
[b] Institute of Public Health of Montenegro, Podgorica, Montenegro
[c] Institute of Technical Sciences of SASA, Belgrade, Serbia
[d] Innovation Centre, Faculty of Technology and Metallurgy, University of Belgrade, Belgrade, Serbia
[e] Faculty of Technology and Metallurgy, University of Belgrade, Belgrade, Serbia
[f] Serbian Academy of Sciences and Arts, Belgrade, Serbia

ARTICLE INFO

Article history:
Received 3 April 2018
Received in revised form 4 September 2018
Accepted 6 October 2018
Available online 8 October 2018

Keywords:
Steel slag
Adsorption
Copper
Alkali activation
Porous materials
FTIR

ABSTRACT

Pristine electric arc furnace slag (EAFS) as well as EAFS modified by alkali activation i.e. alkali activated slag (AAS) have found a novel application as adsorbents used in Cu^{2+} removal from sulfate solutions. The adsorption tests were carried in batch conditions and results have shown that alkali activation of EAFS enhances the Cu^{2+} adsorption. The adsorption process was found to follow a pseudo second-order kinetic model and occurs via formation of posnjakite ($Cu_4(SO_4)(OH)_6{\cdot}H_2O$) on the surface of both, EAFS and AAS. Enhanced adsorption properties of AAS, compared to EAFS, are attributed to a more porous structure, larger specific surface area and an increased number of surface groups involved in the binding of Cu^{2+}.

1. Introduction

The electronics industry generates a large amount of copper bearing sulfate effluent due to the utilization of copper in the production of various electronic components and the use of sulfuric acid as an agent in electroplating, etching, rinsing, chemical and mechanical polishing [1]. This effluent presents a serious risk for the environment, when discharged into soil and inland water without necessary treatment.

Metallurgical slag is considered a highly efficient adsorbent due to the presence of surface species (AlOH, AlO^-, SiOH, SiO^-) which are responsible for heavy metal removal from wastewaters [2]. It is proposed that binding of heavy metals occurs preferentially on silanol (Si-OH) surface sites due to higher content of Si than Al and the interaction of the hydrolysis metal forms with the slag surface can be formulated as follows [2,3]:

$$\geq Si-OH \ \ldots \ H-O-H[Me(OH)_2]_3^{2+} \leftrightarrow Si-OMe + H_3O^+ \qquad (1)$$

Since adsorption properties of slag may be improved by modification [4,5], the aim of this study was to compare the experimental data of Cu^{2+} adsorption from sulfate solutions onto EAFS and AAS. The physicochemical, morphological and mineralogical characteristics of original and modified EAFS, before and after adsorption, were evaluated.

2. Experimental

The main oxide constituents of EAFS used in this study were 46.5% CaO, 23.5% FeO, 12.2% SiO_2, 6.5% MgO, and 7.24% Al_2O_3. The preparation of alkali activated slag (AAS) is described in a previous publication [6]. The slag was alkali activated at solid to liquid mass ratio of 4, using the Na_2SiO_3 solution as an activator. Time and temperature of curring were 48 h and 65 °C, respectively. Both, EAFS and AAS, in powder form, were washed with deionized water and dried at 105 °C. The batch adsorption tests were performed by mixing solid slag samples (either EAFS or AAS) with sulfate solutions containing the Cu^{2+} at a concentration of 100 mg L^{-1} and pH = 5, at solid to liquid ratio of 0.4 for a period of 35 min. After adsorption tests, the solutions were filtered and concentration of

* Corresponding author at: University of Montenegro, Faculty of Metallurgy and Technology, Podgorica, Montenegro.
E-mail address: irena@ac.me (I. Nikolić).

https://doi.org/10.1016/j.matlet.2018.10.027
0167-577X/

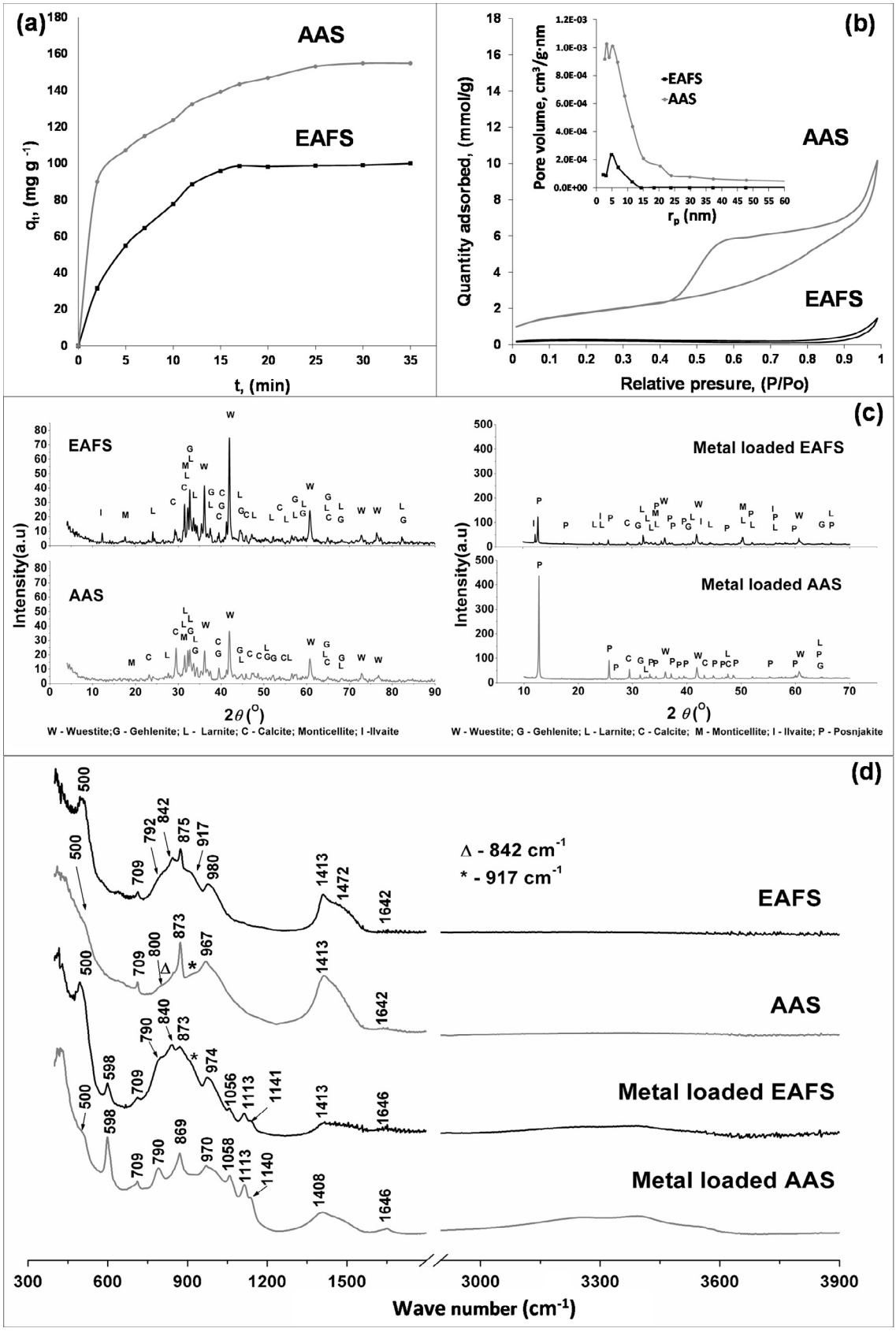

Fig. 1. Effect of contact time on the adsorption of Cu^{2+} onto EAFS and AAS (a); Adsorption/desorption isotherms (inset: pore size distribution) of EAFS and AAS (b); XRD patterns of EAFS and AAS before and after adsorption test (c). FTIR spectra of EAFS and AAS before and after adsorption tests (d).

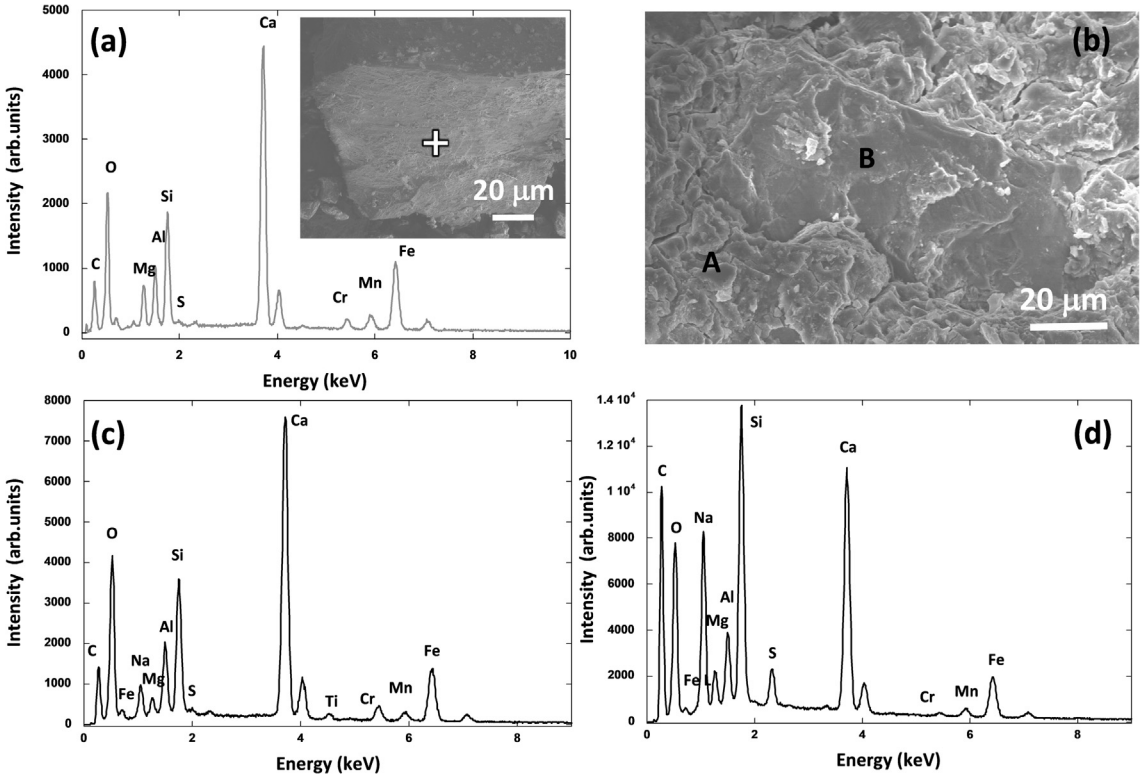

Fig. 2. SEM-EDS of EAFS (a) and AAS (b–d) before adsorption.

Cu^{2+} ions in filtrates were analyzed by inductively coupled plasma-optical emission spectrometry (ICP-OES).

The efficiency of the adsorption process was evaluated through the change in adsorption capacity i.e. the amount of Cu^{2+} uptake by adsorbents (q_t) at any time t (mg g^{-1}), calculated as follows:

$$q_t = \frac{(C_o - C_e)}{m} V \quad (2)$$

where C_0 and C_t are the initial and final concentrations, respectively, of Cu^{2+} in solution, V is the volume of Cu^{2+} ions solution, and m is the dry mass of adsorbent. For the characterization of EAFS and AAS phase composition, morphology, porosity and functional groups on the particles surface, before and after adsorption process, XRD, SEM/EDS, BET and FTIR techniques were used, respectively.

3. Results and discussion

The results of adsorption studies indicated that AAS has a higher adsorption capacity than EAFS (Fig. 1a). The porosity analysis (Fig. 1b) has shown a more pronounced hysteresis loop on the isotherm of AAS in comparison to EAFS, indicating a development of mesoporosity as a result of alkali activation. One peak at around 4.8 nm and two peaks at around 3.3 and 5.2 nm on the differential curves of the pore size distribution of EAFS and AAS, respectively, represent the majority of present mesopores (Fig. 1b inset). It is evident that the pore size was not significantly changed upon alkali activation, but the pore volume was increased. The total pore volume and BET surface area of EAFS were 0.0015 cm^3/g and 0.6 m^2/g while for AAS sample these values were 0.0143 cm^2/g and 6.5 m^2/g, respectively. As it is evident that AAS is the more porous structure, enhanced adsorption is present by facilitating Cu^{2+} permeation into the pores of adsorbent.

The XRD analysis results (Fig. 1c) have shown that EAFS and AAS are mainly X-ray amorphous materials (broad diffraction hump of 2θ from 28 to 38°). In both samples, the main crystal phases were: wuestite (FeO), larnite (Ca_2O_4Si), gehlenite ($Al_2Ca_2O_7Si$), Moreover, small amounts of monticellite ($CaMgSiO_4$), calcite ($CaCO_3$) and ilvaite ($CaFe_3O(OH)(Si_2O_7)$) were present. The new crystal phase, posnjakite ($Cu_4(SO_4)(OH)_6{\cdot}H_2O$) was observed in both EAFS and AAS metal loaded samples which indicated that ***a***dsorption of Cu^{2+} onto each adsorbent is accompanied by the development of posnjakite phase.

The FTIR spectra of EAFS and AAS, before and after adsorption tests, are given in Fig. 1d. The spectrum of EAFS exhibits a band at 500 cm^{-1} ascribed to O-T-O bending modes of TO_4 tetrahedra (T = tetrahedral Si or Al) [7] and bands in the 750–1200 cm^{-1} region ascribed to Si—OH bending (at 842 cm^{-1}), stretching vibrations of Al—O—Si (at 875 cm^{-1}) and Si—O—T (at 792, 917 and 980 cm^{-1}) bonds [8–10]The spectra of AAS sample show the most important changes at 500 cm^{-1} and in the region of 750–1200 cm^{-1} as a result of calcium (alumino) silicate hydrate (C-A-S-H) formation via alkali activation. The two bands that comprise the C-A-S-H were observed in spectra of AAS sample: intense peak at 873 cm^{-1} attributed to Si—OH bending [11] and at 967 cm^{-1} attributed to Si—O stretching vibrations in the SiO_4 tetrahedra [12].

Since the sorption of heavy metals onto the slag in acidic environment preferentially occurs through binding of metals to the silanol group (Si—OH) thereby resulting in the formation of hydrooxocomplexes [3], modification of EAFS by alkali activation enhances adsorption by increasing the number of Si—OH groups. Moreover, in aqueous environment, the water-induced dissociation of the Si—O bonded interactions from C-A-S-H also leads to the formation of Si—OH groups [13] which in turn contribute to the enhanced adsorption of Cu^{2+} ions.

In the spectra of both, EAFS and AAS metals loaded samples, multiple peaks which suggest Cu binding in the form of posnjakite were observed: bands at 598 cm^{-1} and in the range of 1050–1200 cm^{-1} attributed to vibrational modes of SO_4^{2-} groups, band

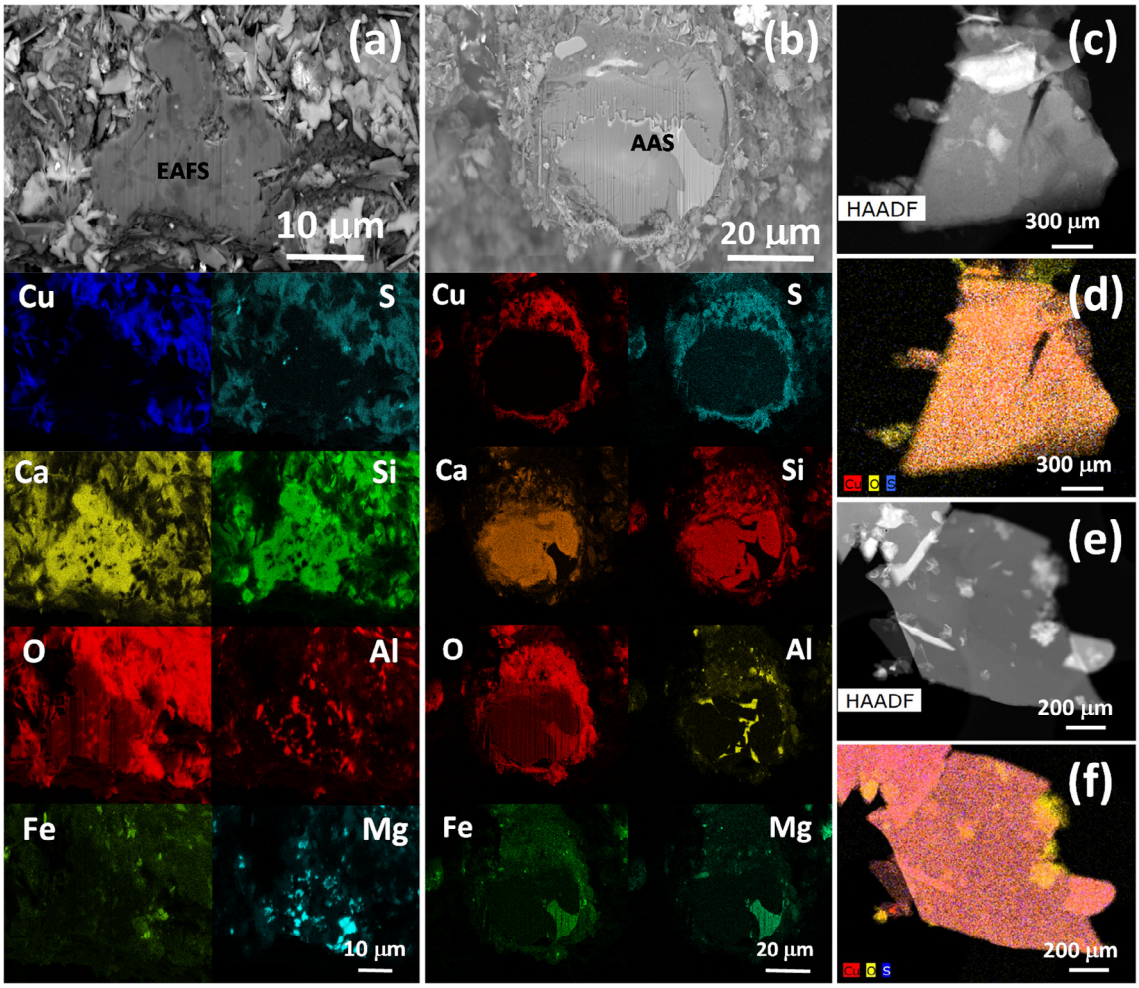

Fig. 3. SEM micrographs of the cross-section of EAFS (a) and AAS (b) after adsorption and appropriate EDS composite maps of elemental distribution; HAADF STEM micrographs with EDS maps of platelets attached on the surface of EAFS (c and d) and AAS (e and f).

at 790 cm^{-1} attributed to Cu—OH bending and a wide band between 3000 and 3700 cm^{-1} attributed to OH vibrations in silanol groups and adsorbed water [14,15]. The bands attributed to vibrational modes of SO_4^{2-} and Cu-OH groups have higher intensity in comparison to the spectrum of metal loaded EAFS, indicating a more effective adsorption of Cu^{2+} by AAS.

Moreover, the spectrum of EAFS and AAS before and after adsorption show small-intensity peak near 1640 cm^{-1} ascribed to H—OH bending of hydroxyl groups and two vibrational modes of CO_3^{2-} at 709 cm^{-1} and in region 1330–1580 cm^{-1}.

The results of ESM-EDS analysis of EAFS and AAS before adsorption are given in the Fig. 2. The structure of AAS (Fig. 2b) comprise of reaction product (region A) and unreacted slag (region B). Much higher Ca and Si content in the region A (Fig. 2d) than in region B (Fig. 2c) indicate formation of C-(A)-S-H as a reaction product of slag alkali activation [16]. SEM images with appropriate EDS maps of EAFS (Fig. 3a) and AAS (Fig. 3b) after adsorption clearly indicate that removal of Cu^{2+} from sulfate solution occur via adsorption since the Cu bearing crystals are adhered on the surface of EAFS and AAS and not through bulky material. Moreover, similar distribution modes were observed for Cu, S and O for both EAFS and AAS samples after adsorption indicating formation of compound containing the Cu, S and O, which is consistent with XRD finings that posnjakite is formed as a result of adsorption process. Scanning transmission electron microscopy (STEM) in high angle annular dark field (HAADF) with EDS maps of elemental distribution Cu, O and S of EAFS (Fig. 3c and d) and AAS (Fig. 3e and f) that Cu and S are more abundant in the AAS than in EAFS confirming the enhanced adsorption properties of AAS.

4. Conclusions

Results obtained in this investigation have shown that AAS exhibits a higher adsorption capacity in comparison to EAFS. This enhanced property of AAS is a result of a more development porosity than EAFS as well as the surface modification of the slag itself. Alkali activation leads to higher pore volume, larger surface area and a larger number of functional groups (Si—OH and Si—O) capable of binding with Cu^{2+} ions on the slag surface, which was accomplished through the formation of posnjakite.

Acknowledgments

The authors would like to acknowledge the support of the Montenegrin Ministry of Science in the framework of Project no. 01-2383/2. VVR and VRR acknowledge the support by the Ministry of Education, Science and Technological Development of the Republic of Serbia, under contract No. III45019 and 172054, respectively. VRR acknowledges support from Serbian Academy of Sciences and Arts, Project #F141.

References

[1] M.K. Jha, N. Van Nguyen, J. Chun Lee, J. Jeong, J.M. Yoo, J. Hazard. Mater. 164 (2009) 948–953, https://doi.org/10.1016/j.jhazmat.2008.08.103.

[2] S.V. Dimitrova, Water Res. 36 (2002) 4001–4008, https://doi.org/10.1016/S0043-1354(02)00120-3.

[3] S.V. Dimitrova, Water Res. 30 (1996) 228–232, https://doi.org/10.1016/0043-1354(95)00104-S.

[4] J. Duan, B. Su, Chem. Eng. J. 246 (2014) 160–167, https://doi.org/10.1016/j.cej.2014.02.056.

[5] L. Bláhová, Z. Navrátilová, M. Mucha, E. Navratilova, V. Neděla, Int. J. Environ. Sci. Technol. 1437 (2017) 1–10, https://doi.org/10.1007/s1376.

[6] I. Nikolić, L. Karanović, I.J. Častvan, V. Radmilović, S. Mentus, V. Radmilović, Mater. Lett. 133 (2014) 251–254, https://doi.org/10.1016/j.matlet.2014.07.021.

[7] G. Ya-min, F. Yong-hao, Y. Duo, G. Yong-fan, Z. Chen-hui, Constr. Build. Mater. 79 (2015) 1–8, https://doi.org/10.1016/j.conbuildmat.2014.12.068.

[8] Z. Liu, G. Qian, J. Zhou, C. Li, Y. Xu, Z. Qin, J. Hazard. Mater. 157 (2008) 146–153, https://doi.org/10.1016/j.jhazmat.2007.12.110.

[9] B. Walkley, R. San Nicolas, M.A. Sani, G.J. Rees, J.V. Hanna, J.S.J. van Deventer, J. L. Provis, Cem. Concr. Res. 89 (2016) 120–135, https://doi.org/10.1016/j.cemconres.2016.08.010.

[10] B.A. Morrow, A.J. McFarlan, J. Phys. Chem. 96 (1992) 1395–1400, https://doi.org/10.1021/j100182a068.

[11] N. Zhang, H. Li, Y. Zhao, X. Liu, J. Hazard. Mater. 306 (2016) 67–76, https://doi.org/10.1016/j.jhazmat.2015.11.055.

[12] F. Puertas, M. Palacios, H. Manzano, J.S. Dolado, A. Rico, J. Rodríguez, J. Eur. Ceram. Soc. 31 (2011) 2043–2056, https://doi.org/10.1016/j.jeurceramsoc.2011.04.036.

[13] A.F. Wallace, G.V. Gibbs, P.M. Dove, J. Phys. Chem. A. 114 (2010) 2534–2542, https://doi.org/10.1021/jp907851u.

[14] M.D. Lane, Am. Mineral. 92 (2007) 1–18, https://doi.org/10.2138/am.2007.2170.

[15] C. Zaffino, V. Guglielmi, S. Faraone, A. Vinaccia, S. Bruni, Spectrochim. Acta – Part A Mol. Biomol. Spectrosc. 136 (2015) 1076–1085, https://doi.org/10.1016/j.saa.2014.09.132.

[16] C.K. Yip, G.C. Lukey, J.S.J. Van Deventer, Cem. Concr. Res. 35 (2005) 1688–1697, https://doi.org/10.1016/j.cemconres.2004.10.042.